The Astrophysical Journal, 629:259–267, 2005 August 10

FORMATION HISTORIES OF DWARF GALAXIES IN THE LOCAL GROUP

Massimo Ricotti[1] and Nickolay Y. Gnedin[2]
Received 2004 August 5; accepted 2005 April 28

ABSTRACT

We compare the properties of dwarf galaxies in the Local Group with the simulated galaxies formed before reionization in a cosmological simulation of unprecedented spatial and mass resolution, including radiative feedback effects. We find that a subset of the Local Group dwarfs are already remarkably similar to the simulated dwarf galaxies in all their properties before reionization. On the basis of this similarity, we propose the hypothesis that Local Group dwarfs form in a variety of ways: some of them are "true fossils" of the pre-reionization era, some of them form most of their stars later, after reionization (we call them "survivors" of the reionization era), and the rest of them form an intermediate group of "polluted fossils." We also identify a simple observational test that is able to test our hypothesis.

Subject headings: cosmology: theory — galaxies: dwarf — galaxies: formation — Local Group — stars: formation

1. INTRODUCTION

Nothing emphasizes our lack of understanding of the origin of the dwarf galaxies of the Local Group more than the well-known "substructure crisis" of the cold dark matter (CDM) paradigm (Klypin et al. 1999; Moore et al. 1999)—the fact that the number of dark matter halos in the Local Group predicted by CDM simulations is much larger than the number of observed Galactic satellites. Several explanations have been suggested so far for resolving the "crisis."

The hypothesis of Bullock et al. (2001)—hereafter the "reionization scenario"—proposed that dwarf spheroidal galaxies (dSphs) in the Local Group formed during the pre-reionization era, and processes of photoionization feedback (Babul & Rees 1992; Efstathiou 1992; Shapiro et al. 1994, 2004; Haiman et al. 1996; Thoul & Weinberg 1996; Quinn et al. 1996; Weinberg et al. 1997; Navarro & Steinmetz 1997; Gnedin 2000b; Dijkstra et al. 2004; Susa & Umemura 2004) resulted in the suppression of star formation below the observable level in 90% of the low-mass dark matter halos populating the Local Group. The reionization scenario is prompted by the fact that almost all Local Group dSphs exhibit a prominent old population and a decline of their star formation rates about 10 Gyr ago. While in the standard ΛCDM theory (Spergel et al. 2003; Tegmark et al. 2004) stellar reionization took place 12.5 Gyr ago, current observational techniques for measuring absolute stellar ages are not able to differentiate between 10 and 12.5 Gyr (e.g., Krauss & Chaboyer 2003). Although the observed drop of star formation rate is consistent with reionization at redshift $z \sim 6$, as noted by Grebel & Gallagher (2004), the metallicity spreads observed in the old populations may imply a star formation history protracted over about 2 Gyr, to redshift $z \sim 3$. In this paper we critically discuss this important issue. We show that our simulations reproduce the observed metallicity spreads without a protracted period of star formation. The metallicity spreads observed in our simulated dwarfs can be understood in terms of hierarchical accretion of subhalos containing stars with different metallicities.

An alternative explanation to the substructure crisis was proposed by Stoehr et al. (2002). According to their hypothesis, dwarf galaxies are hosted in dark matter halos more massive ($\sim 10^9$–$10^{10}\ M_\odot$) than in the reionization scenario. While this idea resolves the "crisis," it does not provide an explanation for the origin of dwarf galaxies.

A more comprehensive and complex picture has been recently proposed by Kravtsov et al. (2004). Under their hypothesis—hereafter the "tidal scenario"—most dwarf galaxies used to be much (up to a factor of 100) more massive during the formation episodes of the Milky Way and Andromeda and thus were not affected by photoionization feedback. They formed most of their stars at $z \sim 3$, but later most of the dark matter was tidally stripped during their evolution within the Milky Way and Andromeda halos. Kravtsov et al. (2004) emphasize that in their model a large variety of star formation histories is observed, and some of the dwarf galaxies do indeed follow the "reionization track," but the bulk of stars in the Local Group dwarfs are formed after reionization.

Thus, the key difference between the reionization and tidal hypotheses is whether most of the stars in a given dwarf galaxy formed in *halos of mass* $\lesssim 10^8\ M_\odot$ before reionization ($z > 6$, 12.5–13 Gyr ago) or in *more massive halos* after reionization, during the epoch of formation of the Milky Way and Andromeda ($z \sim 2$–3, 10–11 Gyr ago).

In this paper we propose that dSphs are fossils of galaxies with mass $M_{\rm dm} < 10^8\ M_\odot$ that formed before reionization, while dwarf Irregular galaxies (dIrrs) formed later in more massive halos. The original contribution of our study is that for the first time we have been able to simulate the first population of galaxies including the relevant feedback processes that are known to self-limit their formation. Before our work (Ricotti et al. 2002a, 2002b), the mainstream wisdom was that negative feedback effects (namely, the rapid photodissociation of H_2) suppress the formation of all galaxies with mass smaller than $10^8\ M_\odot$. We find instead that these galaxies do form, and, at the epoch of their formation, they closely resemble dSphs. This second result is the one we emphasize in this paper. We also show that reionization feedback is not the dominant mechanism that suppresses star formation in most small mass halos. Negative feedback such as photoheating by the stars inside each galaxy and inefficient cooling produce the observed properties of dSphs well before reionization of the intergalactic medium (IGM) is complete.

It is quite surprising that we find such an astonishing agreement between all properties of simulated dwarf galaxies at $z \sim 8$ and dSphs. Our simulations did improve on previous ones but are still far from a complete treatment of the problem that, as we

[1] Institute of Astronomy, Madingley Road, Cambridge CM3 0HA, England; ricotti@ast.cam.ac.uk.
[2] CASA, University of Colorado, Boulder, CO 80309; gnedin@casa.colorado.edu.

briefly illustrate, is not trivial. The efficiency of star formation in the first minihalos with masses $\lesssim 10^8\ M_\odot$ (i.e., virial temperature $T_{\rm vir} \lesssim 10^4$ K) is determined by many competing feedback processes, including the formation and disruption of H_2, metal enrichment, photoevaporation, and supernova (SN) explosions. Since small mass protogalaxies cannot cool by Lyα emission, the presence of H_2 molecules is essential to trigger their initial collapse. We know that H_2 is easily destroyed by far-ultraviolet radiation emitted by the first stars (negative feedback). On the other hand, ionizing radiation and dust production are known to enhance the formation rate of H_2 (positive feedback). Whether efficient star formation is possible in these minihalos depends on which feedback (positive or negative) is dominant. By including three-dimensional radiative transfer of ionizing radiation (Ricotti et al. 2002a) in the simulations, we are able to model two additional types of feedback: the positive feedback for H_2 formation and the photoevaporation of dwarfs from internal sources. As already mentioned, contrary to previous studies, we find that low surface brightness galaxies do form in a fraction of the first minihalos. Reionization does not substantially affect their properties because they have already lost most of their gas due to internal ionizing sources. After reionization, we expect that the formation of small mass galaxies will stop and their stellar populations will evolve only passively. Only the few most massive dwarfs in our simulation retained some of their gas and may continue to form stars after reionization.

In summary, the goal of this paper is to provide evidence in support of the primordial origin of dSphs by comparing the abundant observational data on Local Group dwarfs with the results of detailed numerical simulation of formation of dwarf galaxies in the pre-reionization era. Aside from the origin of dSphs, the aim of study is to improve our understanding of theories of the formation of the first galaxies and answer a longstanding question: how massive were the first galaxies?

2. SIMULATION

The results shown in this work are based on a detailed analysis of the galaxies found in high-resolution cosmological simulations of a cosmological volume during the preionization era. The simulations include dark matter, gas, stars, and the feedback of star formation on gas chemistry and cooling. The main addition with respect to other works (e.g., Machacek et al. 2001; Tassis et al. 2003) is a self-consistent treatment of the spatially inhomogeneous and time-dependent radiative transfer of photons in four frequency bands (H I ionizing radiation, He I and He II ionizing radiation, and optically thin radiation). This allows us to study, in addition to the global feedback effects of the background radiation, the role of internal and local feedback effects. Partially because of the inclusion of a more realistic treatment of radiative feedback, we find that the H_2 photodissociating background is not the dominant feedback and does not stop star formation in minihalos.

The simulation we use in this paper has been thoroughly described in Ricotti et al. (2002a, 2002b) as run "256L1p3." Here we remind the reader that the simulation included 256^3 dark matter particles, an equal number of baryonic cells, and more than 700,000 stellar particles. The mass resolution of our simulation is 900 $M_\odot$ in baryons, and the real comoving spatial resolution (twice the Plummer softening length) is 150 h^{-1} pc (which corresponds to a physical scale of 24 pc at $z = 8.3$). This unprecedented resolution allows us to resolve the cores of all simulated galaxies that would correspond to the observed Local Group dwarfs. The simulation includes most of the relevant physics, including time-dependent, spatially variable radiative transfer,

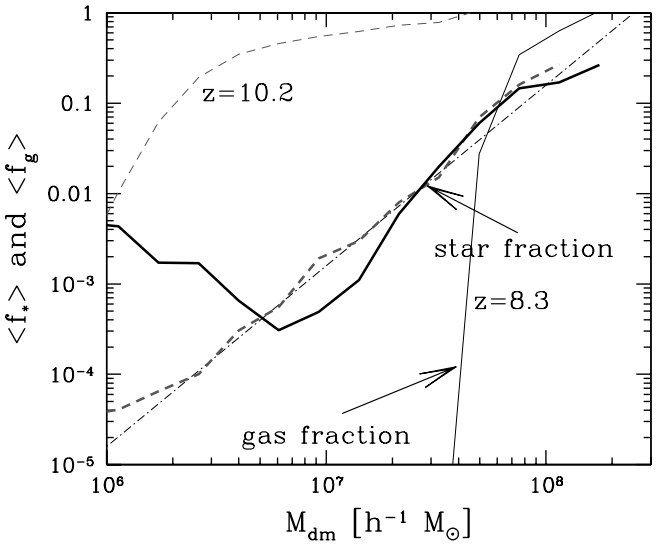

FIG. 1.—Mean gas fraction (*thin solid line*) and the mean stellar fraction (*thick solid line*) as a function of the dark matter mass for the simulated objects at $z = 10.2$ (*dashed lines*) and at the final moment of our simulation, $z = 8.3$ (*solid lines*). Both fractions are normalized by the universal baryon fraction. The dot-dashed line represents a power-law relation $\propto m^2$.

detailed radiative transfer in Lyman-Werner bands, nonequilibrium ionization balance, etc.

In this work, however, we also include the effect of reionization in that simulation. Because the size of the simulation box has been fixed at 1 h^{-1} comoving Mpc, the simulation volume is too small to model the process of cosmological reionization with sufficient accuracy. We therefore assume that the simulation volume is located inside an H II region of a bright galaxy at a higher redshift. Specifically, we introduce a source of ionizing radiation within the computational box, properly biased, which corresponds to a star-forming galaxy with the constant star formation rate of 1 $M_\odot$ yr^{-1} (similar to star formation rates of observed Lyman break galaxies at $z \sim 4$; Steidel et al. 1999). The source is switched on at $z = 9.0$, and by $z = 8.3$ the whole simulation box is completely ionized and star formation in dwarf galaxies has ceased. Because of the computational expense, we have not continued our simulation beyond $z = 8.3$. As mentioned in § 1, the photoevaporation of dwarf galaxies after reionization has been studied extensively. Recent works include those of Shapiro et al. (2004) and Susa & Umemura (2004), which addressed the importance of self-shielding using three-dimensional simulations coupled to one-dimensional radiative transfer (i.e., they assume that the ionizing source is very far from the dwarf galaxy).

Figure 1 shows the mean gas (*thin solid line*) and stellar (*thick solid line*) fractions as a function of the dark matter mass for the objects in our simulation. We show these quantities at redshift $z = 10.2$ (*dashed lines*) and $z = 8.3$ (*solid lines*). Note that the objects with masses below $\sim 10^8\ M_\odot$ contain no gas at the end of our simulation. Most of the small mass galaxies lose all their gas well before reionization, which in our simulation happens between redshift $z \sim 9$ and 8.3. This is the result of gas photoheating by massive stars inside the galaxy and not by the external ionizing background. A remarkable result is that the mean stellar fraction is a time-independent quantity. It is apparent from the figure that the mean stellar fraction as a function of halo mass is well approximated by a power law that does not evolve with redshift (the increase in the stellar fraction for the lowest mass objects is probably an artifact of the limited mass resolution).

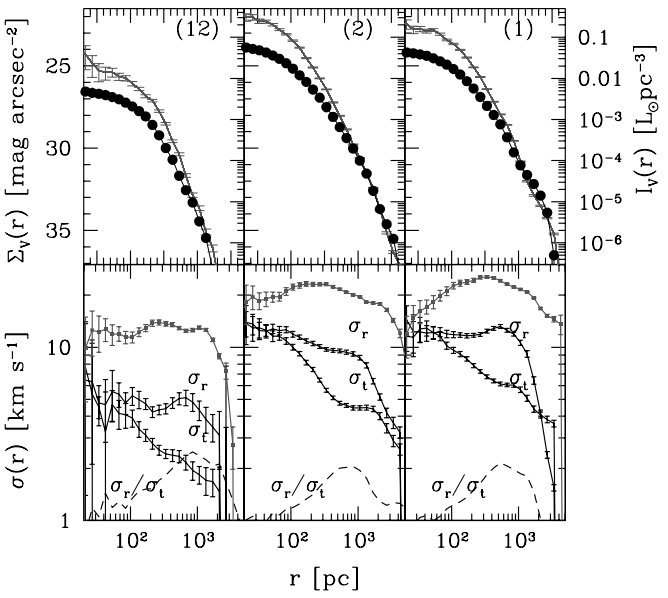

FIG. 2.—Stellar surface (*filled circles*) and volume (*gray lines*) densities (*top row*) and stellar (*black lines*) and dark matter (*gray triangles*) velocity dispersions (*bottom row*) as a function of radius for three representative objects from our simulation at $z = 8.3$. The degree of anisotropy of the velocity dispersion is usually measured by the parameter $\beta = 1 - (\sigma_r/\sigma_t)^{-2}$, where σ_r is the radial velocity dispersion and σ_t is tangential velocity dispersions. The dashed lines in the bottom panels show σ_r/σ_t.

Figure 2 shows radial profiles for three representative and well-resolved objects. In the top panels we show surface (*filled circles*) and volume (*gray lines*) luminosity densities in the V band. The bottom panels show the velocity dispersions for both the dark matter (about 50,000 particles per halo) and stars (about 10,000 particles per halo). Note that stellar velocity dispersions (*black points*) are below that of the dark matter (*gray triangles*) and that stellar orbits are mildly anisotropic in the outer parts. The dashed lines in the bottom panels show σ_r/σ_t, where σ_r and σ_t are the radial and tangential velocity dispersions, respectively.

Clearly, it is a long way to go from $z = 8.3$ to the present day. Therefore, in the rest of this paper, we assume that the stellar component of our galaxies does not change after $z = 8.3$ except due to passive stellar evolution. This hypothesis obviously does not apply to *all* observed dwarfs, but it may apply to *some* of them—as we discuss later. The probability, P, of a galaxy collapsed at redshift $z_{\rm coll}$ to survive to redshift z without being incorporated into a larger object is approximately $P \sim (1+z)/(1+z_{\rm coll})$ (Sasaki 1994). We can therefore estimate that about 10% of the galaxies present in our simulation at $z = 8.3$ may have survived almost unspoiled until today. With this approach, we cannot determine what dark matter mass these galaxies would have by $z = 0$: they can continue accreting[3] the dark matter and then lose a significant fraction of it during their orbital evolution within the parent galaxy halo (in this case, Milky Way or Andromeda). It is therefore important to keep in mind throughout this paper that *we use only the properties of the stellar components of simulated galaxies*. Thus, we cannot make a direct test of the tidal scenario and have to rely on stars to tell us the story of the dark matter.

[3] Note that a dark matter halo that virializes at $z = 10$ by the time it reaches redshift $z = 0$ is about 10 times larger in size and mass even if it did evolve passively without accreting any satellite (i.e., in isolation). This is a consequence of the cosmological evolution of the Hubble constant and mean density of the IGM in which it is embedded (see Gunn & Gott 1972; Ricotti & Wilkinson 2004).

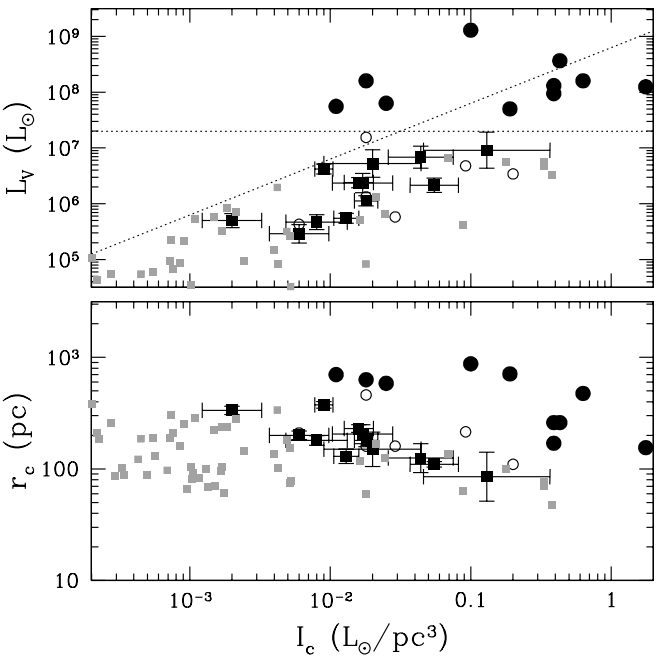

FIG. 3.—V-band luminosity (*top*) and the core radius (*bottom*) vs. the central luminosity density for the Local Group dwarfs (true fossils, *squares with error bars*; polluted fossils, *open circles*; survivors, *filled circles*) and for the simulated galaxies passively evolved to $z = 0$ (*gray squares*). Two dotted lines show two possible boundaries between the fossils and survivors. The data are from Mateo (1998). We have complemented the data using updated distances and photometry from van den Berg (2000) and metallicities and metallicity spreads from Grebel et al. (2003).

In order to predict the luminosities and stellar densities of simulated galaxies at $z = 0$, we need to take into account stellar mass-to-light ratios and stellar evolution. Since the simulated stars would be old by $z = 0$, we adopt a value for the mass-to-light ratio Y as measured in old galactic globular clusters,

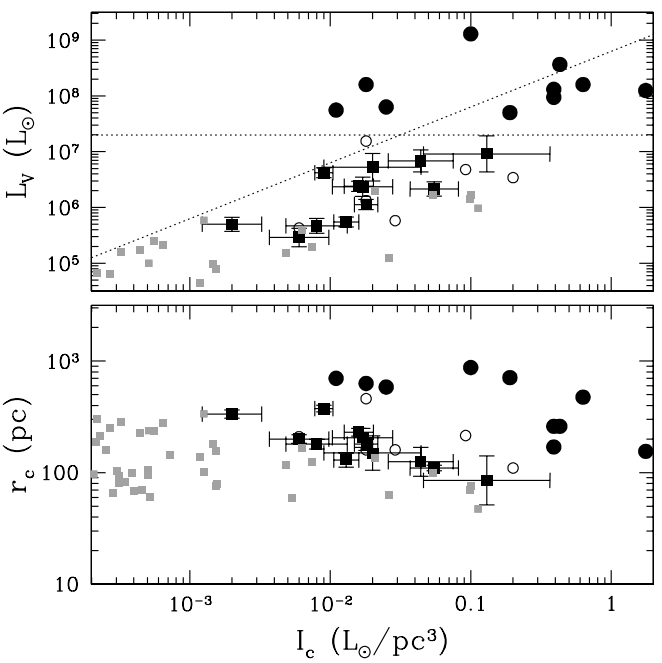

FIG. 4.—Same as Fig. 3, but assuming $M/L_V = 10$ instead of the fiducial value $M/L_V = 3$. The agreement between simulations and data is mildly sensitive to the assumed mass-to-light ratio for all the scaling relationships except the luminosity-metallicity relation, which worsens for larger M/L_V.

$Y \sim 1.5$–2.0 (e.g., Mandushev et al. 1991; Pryor & Meylan 1993). In addition, after some 13 Gyr of stellar evolution, assuming Kroupa initial mass function (IMF) we estimated (using Starburst99; Leitherer et al. 1999) that our stars would lose about 50% of their mass. The exact value depends on the assumed lower mass cutoff of the IMF. Thus, in order to compute the luminosities of the simulated galaxies at $z = 0$, we adopt a fiducial ratio of $M_*(z = 8.3)/L_V(z = 0) = 3$. However, our results are not immensely sensitive to that number—changing it to 2 or 10 would not change our conclusions (see Figs. 3 and 4).

3. RESULTS

The core of the reionization scenario is that some of the Local Group dwarfs are true fossils of the pre-reionization era. Clearly, not all dwarfs fall into this category, since many of them had recent episodes of star formation. But is there a subset of Local Group dwarfs that formed before reionization? We can attempt to answer this question by comparing our simulated dwarfs as they would appear at $z = 0$ with the real observed galaxies. Figure 3 presents such a comparison for the basic structural parameters: the luminosity L_V, the core radius r_c, and the central luminosity density I_c, defined as $I_c = \Sigma_V/2r_c$, where Σ_V is the surface brightness. From the top panel of that figure it is clear that the simulated galaxies, shown by the gray squares without error bars, do not exceed about $10^7\ L_\odot$. Moreover, it appears that the observed galaxies (shown by squares with error bars, open circles, and filled circles; the different symbols are explained later in the text) also fall into two groups—those with luminosities on the order of $10^7\ L_\odot$ and below, and those with luminosities in excess of $5 \times 10^7\ L_\odot$. In addition, these two groups are also clearly separated in the r_c-I_c plane. The low-luminosity dwarfs appear to trace the same distribution as the simulated galaxies, having smaller core radii as the central luminosity density increases. This observation can be understood in terms of the less efficient cooling of the gas in dark matter halos of smaller mass.

Since our simulation has a finite size of the computational box, it is clear that we miss most luminous galaxies forming at the same time as our simulated dwarfs. The tilted dotted line roughly traces the upper envelope of the simulated galaxies, so brighter galaxies that trace the same distribution in the I_c-L_V plane would fall below that line. Some of the observed dwarfs are indeed in this region, but as the bottom panel of Figure 3 shows, their core radii are somewhat larger than those of the simulated galaxies. Thus, we can be confident that we do not miss a large fraction of more luminous dwarfs in our simulation that follow the same distribution as the faint ones. It does not, of course, mean that there should be no more luminous galaxies in a simulation with a larger volume; they will be present, but most of them will have masses in excess of $10^8\ M_\odot$. Therefore, because they will collapse via atomic line cooling, they should have a very different internal structure and be much less susceptible to losing their gas after reionization. Figure 4 is the same as Figure 3, but we assume $M/L_V = 10$ instead of the fiducial value $M/L_V = 3$. The purpose of this figure is to show that our results are robust and almost independent of the assumed M/L_V ratio.

It is therefore tempting to hypothesize that the two groups of low- and high-luminosity dwarfs correspond to two distinct formation tracks—the low-luminosity ones are the "fossils" of the pre-reionization era and the high-luminosity ones formed their stars via atomic line cooling perhaps via the Kravtsov et al. (2004) scenario, as tidally stripped more massive halos (for lack of a better name, we call them "survivors" of the reionization era).

We can now see how our separation of these two groups (based only on the luminosity) compares with the available data on the star formation history of observed dwarfs. Hereafter, we adopt the star formation histories compiled by Grebel & Gallagher (2004). It is well known that almost all dwarfs, in addition to a more or less prominent old population, clearly show some more recent star formation. Therefore, taken at face value, our hypothesis does not hold in comparison with the data. However, it is unreasonable to assume that *all* of the galaxies that formed during the pre-reionization era formed absolutely no stars afterward. Some of them should surely continue accreting dark matter, becoming more massive and switching from the "reionization" track to the "tidal" track. To be more specific, the ability of a dark matter halo to accrete fresh intergalactic gas is controlled by the filtering mass (Gnedin 2000b). In the standard ΛCDM theory the filtering mass increases with time, as does the mass of an individual dark matter halo. Thus, the question of whether a given halo is able to accrete fresh gas after reionization (and, presumably, form new stars) depends on whether its mass grows faster or slower than the filtering mass. We can therefore expect that some of the galaxies that formed before reionization will form no new stars, and some of them will form more stars as they fall into the Milky Way or Andromeda halo and their local filtering mass and accretion history vary. The specific rate with which the gas is reaccreted must depend on the details of a satellite orbit, as has been emphasized by Kravtsov et al. (2004), and so a large variety of possible star formation histories is expected, in qualitative agreement with the observational data. A much more advanced simulation than the one presented here will be required, however, to check whether a quantitative agreement between the theory and the data holds—for example, whether the relative fractions of dwarfs with different star formation histories are consistent with the data.

As mentioned in § 1, another problem faced by the fossil hypothesis is the large metallicity spreads observed in dwarfs with a dominant old population. Grebel & Gallagher (2004) have suggested that these large spreads are not compatible with star formation protracted over a period of <1 Gyr (the time elapsed before reionization). They therefore conclude that star formation in old dwarfs was not affected by reionization. In defense of the fossil hypothesis, we show as part of our analysis that the metallicity spreads in our simulated dwarfs are consistent with observations. Note that star formation in these dwarfs was protracted for <1 Gyr. Our result is probably due to accretion of stars from satellites with different metallicities and would not be captured by any standard chemical evolutionary model.

In order to schematically separate the observed dwarfs in groups according to their star formation histories, we call those dwarfs that formed few (say, $<30\%$) stars after reionization "true fossils," and those that did form a substantial amount of stars "polluted fossils." The various symbols in Figure 3 and the subsequent figures correspond to these classes: true fossils are shown with filled squares with error bars and polluted fossils are shown with open circles. Galaxies with dominant younger stellar populations (they mostly are dIrrs) are shown with larger filled circles and we call them survivors. For the last two groups the error bars are not shown for the sake of clarity. All the galaxies in our simulation have almost identical properties to the true fossils and most polluted fossils. All these galaxies have a prominent old stellar population, as expected. Instead, all the galaxies with a prominent young population (*filled circles*) are part of a distinct population that is not present in our simulation.

Figure 5 presents a separation of the Local Group dwarfs into these three types. Galaxies identified as survivors can be thought of as those dwarfs that formed after reionization (or mostly after reionization) and for which the total mass exceeded the local

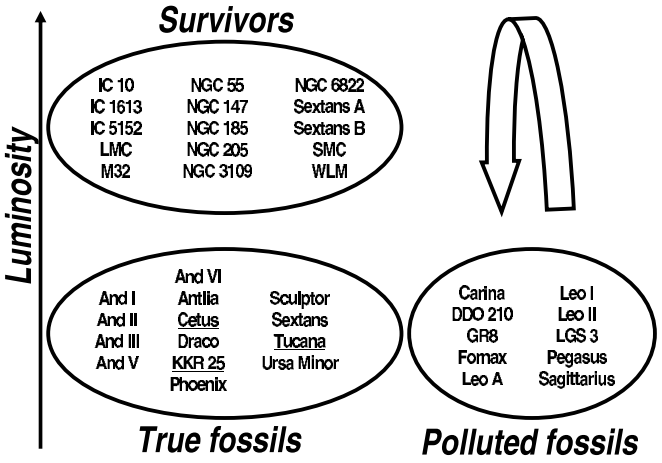

FIG. 5.—Tentative separation of all Local Group dwarfs as well as other nearby dwarfs into three groups: survivors, which formed via the tidal scenario (mostly dIrrs), true fossils, which formed via the reionization scenario, and polluted fossils, which went through both stages. In our tentative classification, most dSphs (14) are true fossils: five are M31 satellites, six are Milky Way satellites, and three (the underlined names) are isolated from both M31 and the Milky Way.

filtering mass at some moment during their evolution. Polluted fossils formed a significant fraction of their stars in the pre-reionization era but also exceeded the local filtering mass at some point in their history. The true fossils formed most of their stars in the pre-reionization era. As a weak argument in favor of this hypothesis, we note that polluted fossils are, on average, brighter than the "true" ones.

This separation of galaxies into individual classes is in some cases rather artificial. For example, both Sextans and Fornax had some recent star formation. We labeled Sextans a true fossil because this recent episode was very small, while Fornax had a factor of 3–4 more stars formed after reionization and thus is labeled a polluted fossil. On the basis of their star formation history, Leo A and Leo I could also be classified as low-luminosity survivors.

In order to support our conclusion, we consider other properties of the simulated and real galaxies. Figure 6 shows the comparison between the data and the simulation for the relation

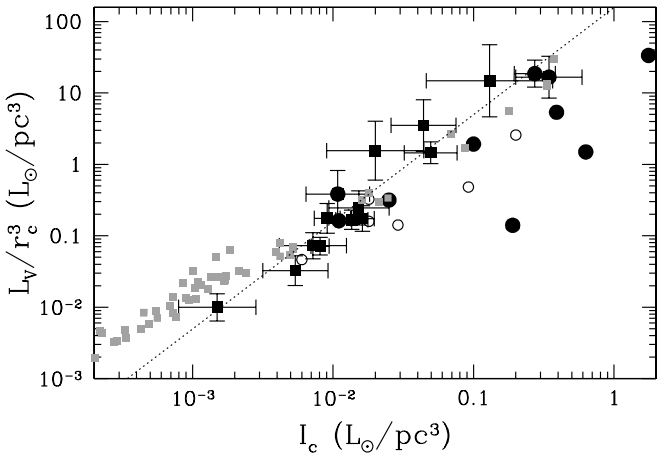

FIG. 6.—*V*-band luminosity per cube of the core radius vs. the central luminosity density for the Local Group dwarfs and for the simulated galaxies (*gray squares*). Filled black squares mark true fossils, open circles mark polluted fossils, and filled circles show survivors. The dotted line shows the power-law fit to the true fossils with the slope fixed to 3/2 (see Gnedin 2000a for details).

between L_v/r_c^3 and I_c, discussed in Gnedin (2000a). We find a scaling relationship

$$\frac{L_v}{I_c r_c^3} \approx 100\left(\frac{I_c}{1\ L_\odot\ \mathrm{pc}^{-3}}\right)^{0.5},$$

shown by the dotted line. If the interpretation of Gnedin (2000a) of this relation is correct, then it simply reflects the Schmidt law for star formation on scales of hundreds of parsecs; in that case the agreement between the data and the simulation is by construction, rather than the success of the model. The star formation in the simulation is assumed to follow the Schmidt law (1.5 slope in the relation between the star formation rate and gas density), and the amplitude is fixed by observational constraints. On the other hand, this agreement does support the reionization scenario because survivors do not follow this tight relation, which could be expected if their stars formed in several independent bursts.

Note that $L_v/(I_c r_c^3)$ is the ratio of the total luminosity to the core luminosity and is therefore a measure of how concentrated the light of the dwarf galaxy is. This ratio is <10 for dSphs like Draco and Ursa Minor ($I_c \sim 5\times10^{-3}\ L_\odot\ \mathrm{pc}^{-3}$) and is almost 100 for dwarf elliptical galaxies (dEs) like NGC 205 and NGC 147 ($I_c \sim 1\ L_\odot\ \mathrm{pc}^{-3}$). The galaxies that we classified as survivors have central luminosity density generally comparable to dEs but less concentrated light profiles. We do not observe such objects in our simulation, despite the fact that cores of these galaxies, if they were present in the simulation, would be completely resolved.

Figure 7 compares the surface brightness and the core radii of simulated and observed galaxies as a function of the luminosity. The simulation reproduces very well the structural properties and scaling relations of the galaxies that we classified as true fossils. The lines show, for comparison, the scaling relations derived by Kormendy & Freeman (2004) for more luminous late-type galaxies (Sc-Im) with luminosities in the range $10^8\ L_\odot \lesssim L_B \lesssim 10^{11}\ L_\odot$.

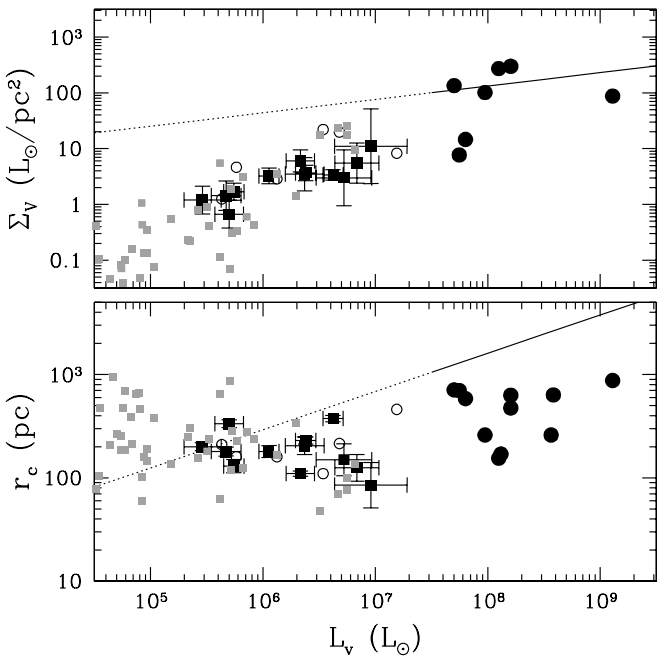

FIG. 7.—Surface brightness (*top*) and core radius (*bottom*) as a function of the *V*-band luminosity for the simulated and observed dwarfs. Symbols are the same as in Fig. 6. For comparison, we show (*solid lines*) the scaling relationships for the more luminous Sc-Im galaxies ($10^8\ L_\odot \lesssim L_B \lesssim 10^{11}\ L_\odot$) derived by Kormendy & Freeman (2004).

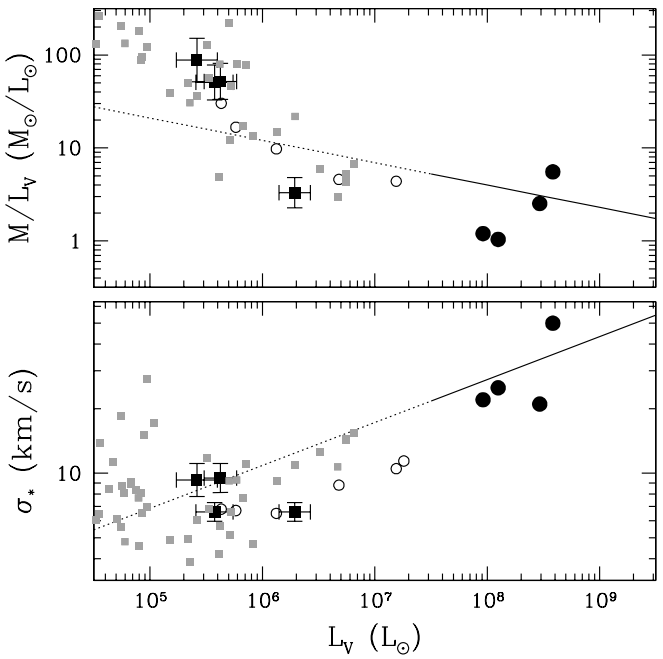

FIG. 8.—Total mass-to-light ratio (*top*) and stellar velocity dispersion (*bottom*) for the simulated and observed dwarfs. Symbols and lines are the same as in Fig. 6. Fewer data points appear in this figure because the data do not exist for all Local Group dwarfs.

Figure 8 compares the dynamical state of these galaxies: the stellar velocity dispersion and the total mass-to-light ratio. The latter quantity for the simulated galaxies is computed in the same way as the observed ones ($M/L = 136\sigma_*^2 r_c/L$; see Mateo 1998) and is not taken from the simulations because, as we have mentioned above, there is no simple way to relate the dark matter mass of simulated galaxies at $z = 8.3$ with their dark matter masses at $z = 0$. For comparison, the solid lines show the same scaling relations for late-type galaxies (Kormendy & Freeman 2004). Within the errors, the σ-L_v relation seems to be the same power law for all the galaxy types, but true fossils obey a steeper relationship between the mass-to-light ratio and luminosity than dIrr and Sc-Im galaxies.

Figure 9 gives yet another comparison between the simulation and the data—the metallicity as a function of stellar luminosity. The agreement between stellar metallicities in the simulation and the data is somewhat worse: while the spread in the distribution is consistent with the data, simulated galaxies are more metal-rich by about a factor of 1.5–2. At this point we are not worried by this disagreement as our simulation is not sophisticated enough to predict the stellar metallicities to within a factor of 2. There are several physical and numerical effects that lead to overestimated stellar metallicities in the simulations, such as preferential ejection by supernovae of metal-enriched gas (Mac Low & Ferrara 1999), imperfect mixing of the supernova ejecta on scales not resolved by a simulation, reduced gas accretion on the simulated galaxies due to a limited size of the computational box, etc.

Low-metallicity stars can be produced in two different ways: either by inefficient star formation combined with continuous gas loss or in a single short burst. The first scenario is consistent with the properties of dSphs that have an extended low surface brightness stellar component. The second scenario is usually associated with a higher efficiency of star formation, which results in a more concentrated light profile than the one observed in dSphs, and is probably more appropriate to explain the metal enrichment of globular cluster and dE galaxies.

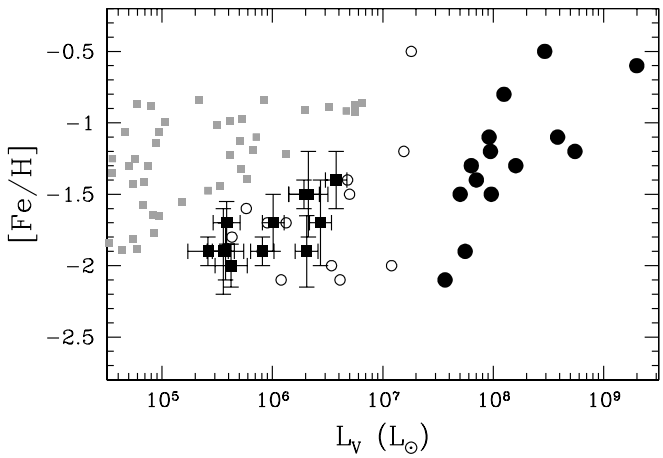

FIG. 9.—Stellar metallicity for the simulated and observed galaxies. Symbols are the same as in Fig. 6. We adopt solar abundances and yield $y = \rho_Z/\rho_* = 1\,Z_\odot$.

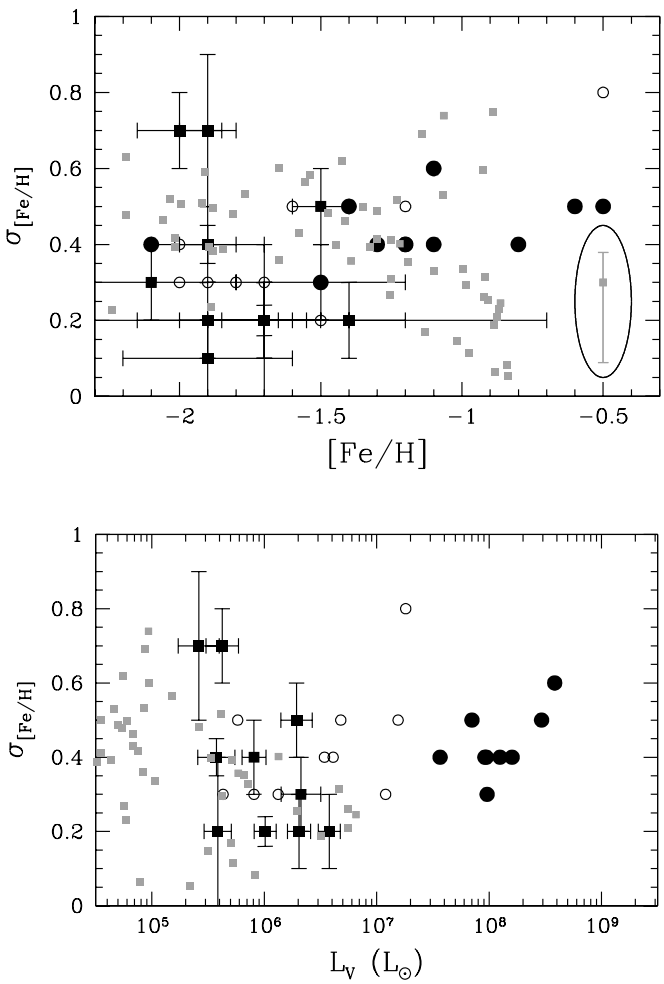

FIG. 10.—Metallicity spread of the stellar populations $\sigma_{[Fe/H]}$, as a function of mean metallicity [Fe/H] for the simulated (*gray squares*) and observed dSphs (symbols are the same as in Fig. 6). The spread $\sigma_{[Fe/H]}$ is defined as the variance of the number-weighted metallicity distribution of the "stellar particles" in each dwarf. A rough estimate of the uncertainty on the metallicity spread is shown by the circled error bar in the bottom right corner. The error is estimated as the mean difference between $\sigma_{[Fe/H]}$ using the mass-weighed and the number-weighed metallicity distributions.

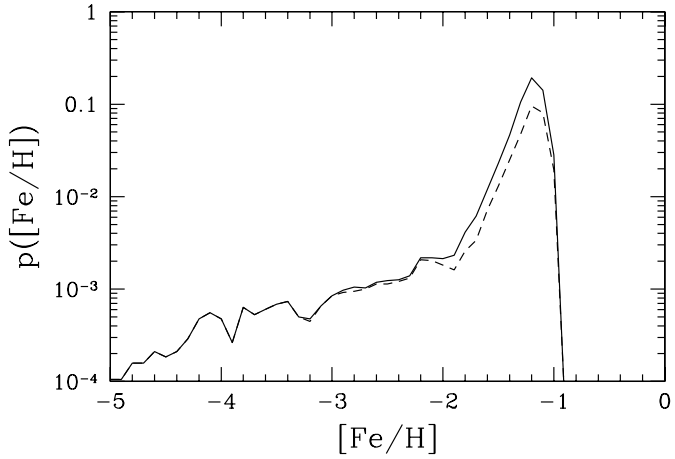

FIG. 11.—Stellar metallicity distribution of one simulated galaxy. The solid and dashed lines show the number- and mass-weighted distributions, respectively.

We have already anticipated that our simulation reproduce the large metallicity spreads observed in dSphs. In Figure 10 we show a comparison between the simulated and the observational data for the metallicity spreads, $\sigma_{[Fe/H]}$, both as a function of the mean metallicity [Fe/H] (*top panel*) and as a function of luminosity L_V (*bottom panel*). We find that the typical metallicity variance in each dwarf is about 0.5 dex, in good agreement with observations. The star formation history in simulated dwarfs is characterized by multiple instantaneous starbursts extended over a period of 0.5–1 Gyr. The starbursts often do occur at almost the same time but in distinct dark matter subhalos that are in the process of merging to form a more massive dwarf. The accretion of stars from the hierarchical distribution of subhalos partially explains the large metallicity spread that we find in our simulation.

Thus, we conclude that the large metallicity spread observed in the old stellar population of dSphs is not a definite signature of star formation extended over 2–4 Gyr (Ikuta & Arimoto 2002; Grebel & Gallagher 2004). Neither the argument based on the long timescale (e.g., 1–4 Gyr) needed to have a substantial iron production by Type Ia SNe is a strong argument in favor of prolonged star formation. The typical timescale for iron enrichment by Type Ia SNe is uncertain and is very likely dependent on the mode of star formation. Matteucci & Recchi (2001) estimated that this timescale varies from 40 to 50 Myr for an instantaneous starburst to 0.3 Gyr for a typical elliptical galaxy to 4–5 Gyr for a disk of a spiral galaxy like the Milky Way. The often-quoted 1 Gyr timescale is based on observations of [α/Fe] versus [Fe/H] in the solar neighborhood stars and is not a universal value. A more detailed study would be needed to derive accurate metal abundance ratios based on the star formation and merger histories found in the simulations. This is beyond the aim of this paper, but it is worth pursuing in a separate study.

We also study the stellar metallicity distribution in each one of our simulated dwarfs. Figure 11 shows such an example. The solid and dashed lines show the number- and mass-weighted distributions, respectively. The metallicity distribution is skewed toward low metallicities, but only a small fraction of the stars, having metallicities $<10^{-4}\,Z_\odot$, could be defined as Population III stars.

4. DISCUSSION

In this paper we have proposed that dwarf galaxies of the Local Group (and, by implication, all other dwarf galaxies in the universe) formed in three different evolutionary paths:

1. True fossils formed most of their stars in the pre-reionization era and have had little (say, <30%) star formation since then.
2. Polluted fossils started as true fossils but had substantial episode(s) of subsequent star formation as they continued accreting mass and were tidally shocked during the formation of the parent galaxy halo.
3. Survivors started forming stars mostly after reionization.

This conclusion is motivated by considering star formation histories of Local Group dwarfs and by comparing their properties with properties of simulated galaxies that formed all their stars before cosmological reionization. The fact that our simulated galaxies are remarkably similar to the subset of the Local Groups dwarfs that we identified as true fossils in Figure 5 renders support to our conclusions. This subset includes almost all known dSphs.

To avoid confusion, it is worth noting that the structural properties of the galaxies that we call true fossils are the result of feedback processes in action prior to reionization. The effect of reionization is simply to preserve those properties by suppressing the star formation rate in halos with masses that remain smaller than the filtering mass in the IGM. In this sense our model differs from the standard "reionization" scenario for the formation of dwarf galaxies.

How would one test this hypothesis? For example, the main argument of Kravtsov et al. (2004) for the tidal origin of the majority of Local Group dwarfs is their preferential location close to the parent galaxy. However, true fossils, living in the oldest dark matter halos of their mass, are highly biased and are also preferentially located closer to the center of the parent halo. Moreover, there are at least two examples of dSphs that are quite far from massive galaxies: Cetus and Tucana, and perhaps the newly discovered Apples 1 (Pasquali et al. 2005).

A more powerful test is based on our conclusion that survivors form later than the true fossils. While measuring absolute ages of dwarf galaxies to 1 Gyr precision is not possible at the moment, determining the *relative* difference of about 1 Gyr in age between two galaxies observed by a uniform technique may, in fact, be possible for a specific range of metallicities and ages using the so-called horizontal branch index (G. Gilmore 2004, private communication; also see Zinn 1993; Harbeck et al. 2001; Mackey & Gilmore 2004); younger galaxies have redder horizontal branch for the same metallicity, although how precise the horizontal branch index method is and the role of the so-called second parameter effect is still a matter of debate.

Luckily, some of the Local Group dwarfs fall into that range of parameters. For example, two galaxies of our true fossil group—And I and And II—have [Fe/H] ≈ -1.5, similar to the iron abundance in two of the survivors—WLM and NGC 3109 (having pairs of galaxies with the same metallicity is absolutely crucial, as even small differences in metallicities can obscure large differences in age). Thus, we can make a prediction that most of the stars that formed in the first burst of star formation in WLM and NGC 3109 should be about 1.5 Gyr younger than most of the stars in And I and And II. The color-magnitude diagrams of And I, And II, and WLM are measured down to $V > 26$, well below the horizontal branch (Da Costa et al. 2002; Rejkuba et al. 2000), although to the best of our knowledge, no photometry down to that levels exists for NGC 3109. Visual comparison of the horizontal branch morphologies for the first three galaxies indicate that And I and And II are indeed substantially older than WLM; also a more rigorous, quantitative test is required to confirm the visual impression. Such a comparison would be a crucial test of our hypothesis—if it is found

that And I and And II are not substantially older than WLM and NGC 3109, that would imply that they are not true fossils, and by inference, few other dSphs are. The main problem that affects this method when comparing the old populations of dSphs to dIrrs is that normally dIrrs have mixed populations, and the overlap between the blue horizontal branch and the young main sequence make it difficult to derive reliable horizontal branch morphology indices in dIrrs. Perhaps a more reliable and accurate relative age indicator is the main-sequence turnoff. The internal accuracy can be better than 1 Gyr in a few nearby dwarfs with photometric data that extend below the main-sequence turnoff.

Using available data, Grebel & Gallagher (2004) address the impact of reionization on the star formation histories of dwarf galaxies. They conclude that most or all dwarf galaxies present an old population that is coeval with the oldest Milky Way populations. They also find that all of the Local Group dwarf galaxies exhibit considerable abundance spreads even within their old populations, indicating that star formation did not occur in a single burst but in episodes that must have extended over several Gyr, well beyond reionization. In this paper we have argued that the observed metallicity spreads are not necessarily an indication of star formation extended over several Gyr. In our simulations all the dwarfs that form before reionization have metallicity spreads consistent with observations. The large iron abundances in dSphs have also been used as an argument in favor of an extended star formation. This is because the timescale for iron enrichment is often assumed to be longer than 1 Gyr. But we point out that this assumption may be true for a continuous mode of star formation but is not necessarily universally true. The timescale depends on the star formation history and could be as short as 50 Myr for a bursting mode of star formation (Matteucci & Recchi 2001).

In principle, $[\alpha/\mathrm{Fe}]$ ratio could be used to discriminate between star formation histories consisting of a single burst or a more prolonged episode of star formation. At the moment, it is not clear how much this test could distinguish true fossils from survivors, since both are expected to have the main burst of star formation for a relatively short period of time. The star formation rate in the true fossils should decrease substantially after reionization. In addition, our simulations show that they have a very peculiar mode of star formation characterized by multiple short bursts (about 10–100 Myr long). It is unclear to us how this mode of star formation may affect their $[\alpha/\mathrm{Fe}]$ ratio and be used as a discriminant. Using existing data on $[\alpha/\mathrm{Fe}]$ ratios in dSphs (Tolstoy et al. 2003; Venn et al. 2004), it might be possible to distinguish between different star formation and enrichment histories, but this would require a more detailed modeling that is beyond the aim of this paper.

In addition, we find that the most massive end of the true fossil population in our simulation [with mass $M > (1\text{–}2) \times 10^8\ M_\odot$] retains a fraction of their gas even after reionization (see Fig. 1). These few "transition" objects may continue forming stars for a while after reionization and have a more extended period of star formation with respect to the rest of the "fossil" population.

To conclude, we would like to emphasize another exciting possibility. From the results of our simulations, we feel quite confident in predicting the existence of fainter and lower surface brightness galaxies than the one currently discovered (see the gray squares at the extreme left corners in Figs. 3, 6, and 7). Two promising candidates for such a class of dwarf galaxies were recently discovered in M31 and near the Milky Way (Zucker et al. 2004; Willman et al. 2005).

Although the detection of such objects in the Milky Way is very difficult, if not impossible, using photometric techniques (due to contamination from foreground stars), in the future it might become possible to search for these objects using spectroscopic techniques by measuring the radial velocities of many stars. Any observation able to put constraints on properties of the faintest bound object in the Local Group would be of extreme interest not only for understanding galaxy formation in the early universe but, more importantly, for uncovering the properties of the elusive dark matter particles.

We are grateful to the anonymous referee for very useful comments that led to great improvement of the original manuscript. We thank R. Wyse, G. Gilmore, A. Kravtsov, O. Gnedin, and J. P. Ostriker for valuable discussions and important insights. M. R. was supported by a PPARC theory grant. This work was supported in part by *HST* Theory grant HST-AR-09516.01-A, NSF grant AST-0134373, and by the National Computational Science Alliance under grant AST 02-0018N and utilized IBM P690 array at the National Center for Supercomputing Applications.

REFERENCES

Babul, A., & Rees, M. J. 1992, MNRAS, 255, 346
Bullock, J. S., Kravtsov, A. V., & Weinberg, D. H. 2001, ApJ, 548, 33
Da Costa, G. S., Armandroff, T. E., & Caldwell, M. 2002, AJ, 124, 332
Dijkstra, M., Haiman, Z., Rees, M. J., & Weinberg, D. H. 2004, ApJ, 601, 666
Efstathiou, G. 1992, MNRAS, 256, 43P
Gnedin, N. Y. 2000a, ApJ, 535, L75
———. 2000b, ApJ, 542, 535
Grebel, E. K., & Gallagher, J. S. 2004, ApJ, 610, L89
Grebel, E. K., Gallagher, J. S., & Harbeck, D. 2003, AJ, 125, 1926
Gunn, J. E., & Gott, J. R. I. 1972, ApJ, 176, 1
Haiman, Z., Rees, M. J., & Loeb, A. 1996, ApJ, 467, 522
Harbeck, D., et al. 2001, AJ, 122, 3092
Ikuta, C., Arimoto, N. 2002, A&A, 391, 55
Klypin, A., Kravtsov, A. V., Valenzuela, O., & Prada, F. 1999, ApJ, 522, 82
Kormendy, J., & Freeman, K. C. 2004, in IAU Symp. 220, Dark Matter in Galaxies, ed. S. D. Ryder et al. (San Francisco: ASP), 377
Krauss, L. M., & Chaboyer, B. 2003, Science, 299, 65
Kravtsov, A. V., Gnedin, O. Y., & Klypin, A. A. 2004, ApJ, 609, 482
Leitherer, C., et al. 1999, ApJS, 123, 3
Machacek, M. E., Bryan, G. L., & Abel, T. 2001, ApJ, 548, 509
Mac Low, M., & Ferrara, A. 1999, ApJ, 513, 142
Mackey, A. D., & Gilmore, G. F. 2004, MNRAS, 355, 504
Mandushev, G., Staneva, A., & Spasova, N. 1991, A&A, 252, 94
Mateo, M. 1998, ARA&A, 36, 435
Matteucci, F., & Recchi, S. 2001, ApJ, 558, 351
Moore, B., Ghigna, S., Governato, F., Lake, G., Quinn, T., Stadel, J., & Tozzi, P. 1999, ApJ, 524, L19
Navarro, J., & Steinmetz, M. 1997, ApJ, 478, 13
Pasquali, A., Larsen, S., Ferreras, I., Gnedin, O. Y., Malhotra, S., Rhoads, J. E., Pirzkal, N., & Walsh, J. R. 2005, AJ, 129, 148
Pryor, C., & Meylan, G. 1993, in ASP Conf. Ser. 50, Structure and Dynamics of Globular Clusters, ed. S. G. Djorgovski & G. Meylan (San Francisco: ASP), 357
Quinn, T., Katz, N., & Efstathiou, G. 1996, ApJ, 278, 49
Rejkuba, M., Minniti, D., Gregg, M. D., Zijlstra, A. A., Alonso, M. V., & Goudfrooij, P. 2000, AJ, 120, 801
———. 2002a, ApJ, 575, 33
———. 2002b, ApJ, 575, 49
Ricotti, M., & Wilkinson, M. I. 2004, MNRAS, 353, 867
Sasaki, S. 1994, PASJ, 46, 427
Shapiro, P. R., Giroux, M. L., & Babul, A. 1994, ApJ, 427, 25
Shapiro, P. R., Iliev, I. T., & Raga, A. C. 2004, MNRAS, 348, 753
Spergel, D. N., et al. 2003, ApJS, 148, 175
Steidel, C. C., Adelberger, K. L., Ciavalisco, M., Dickinson, M., & Pettini, M. 1999, ApJ, 519, 1
Stoehr, F,. White, S. D. M., Tormen, G., & Springel, V. 2002, MNRAS, 335, L84
Susa, H., & Umemura, M. 2004, ApJ, 600, 1
Tassis, K., Abel, T., Bryan, G. L., & Norman, M. L. 2003, ApJ, 587, 13

Tegmark, M., et al. 2004, Phys. Rev. D, 69, 3501
Thoul, A. A., & Weinberg, D. H. 1996, ApJ, 465, 608
Tolstoy, E., Venn, K. A., Shetrone, M., Primas, F., Hill, V., Kaufer, A., & Szeifert, T. 2003, AJ, 125, 707
van den Bergh, S. 2000, PASP, 112, 529
Venn, K. A., Irwin, M., Shetrone, M. D., Tout, C. A., Hill, V., & Tolstoy, E. 2004, AJ, 128, 1177
Weinberg, D. H., Hernquist, L., & Katz, N. 1997, ApJ, 477, 8
Willman, B., et al. 2005, ApJ, 626, L85
Zinn, R. 1993, in ASP Conf. Ser. 48, The Globular Clusters–Galaxy Connection, ed. G. H. Smith & J. P. Brodie (San Francisco: ASP), 302
Zucker, D. B., et al. 2004, ApJ, 612, L121